

# Synthesis of Single-Crystalline Silicon Nitride Nanobelts Via Catalyst-Assisted Pyrolysis of a Polysilazane

Weiyu Yang,<sup>1</sup> Zhipeng Xie,<sup>1</sup> Hezhuo Miao,<sup>1</sup> Ligong Zhang,<sup>2</sup> Hang Ji,<sup>3</sup> and Linan An<sup>\*,†,4</sup>

<sup>1</sup>State Key Laboratory of New Ceramics and Fine Processing, Tsinghua University, Beijing 100084, China

<sup>2</sup>Laboratory of Excited State Process, Changchun Institute of Optics, Fine Mechanics and Physics, Chinese Academy of Sciences, Changchun, China

<sup>3</sup>School of Physics, Peking University, Beijing 100871, China

<sup>4</sup>Advanced Materials Processing and Analysis Center, University of Central Florida, Orlando, Florida 32816

Recently, one-dimensional nanostructures have attracted extensive attention since they are potentially important for both applications and fundamental research. In this paper, we report the synthesis of ultra-long single crystal Si<sub>3</sub>N<sub>4</sub> nanobelts via catalyst-assisted pyrolysis of polymeric precursors. The obtained products contain both  $\alpha$ - and  $\beta$ -Si<sub>3</sub>N<sub>4</sub> nanobelts, which are 50–100 nm in thickness, 400–1000 nm in width, and a few hundreds of micrometers to several millimeters in length. Different from previous techniques for synthesizing one-dimensional structures, the current nanobelts are synthesized through confined crystallization of an amorphous phase. A solid–liquid–gas–solid reaction/crystallization growth mechanism is proposed. The formation of nanobelts instead of nanowires is attributed to the anisotropy growth at an earlier stage.

## I. Introduction

THE discovery of carbon nanotube has stimulated tremendous interest in the synthesis of various one-dimensional nanostructures such as nanotubes, nanorods, nanowires, and nanobelts.<sup>1,2</sup> Due to their seamless structures and dimensional confinement on electron motion, this new class of materials generally possesses unique and superior properties compared to their bulky counterparts.<sup>1,2</sup> Consequently, one-dimensional nanostructures are promising for synthesizing new kinds of multifunctional nanocomposites and nanodevices.<sup>2–6</sup> In addition, this new class of materials also offers a unique opportunity for the fundamental study of dimensional confining phenomena and crystal growth.

Due to its excellent mechanical and thermal properties, Si<sub>3</sub>N<sub>4</sub> is an important engineering material for high-temperature structural applications.<sup>7,8</sup> In addition, Si<sub>3</sub>N<sub>4</sub> is also a wide band gap (5.3 eV) semiconductor in which midgap levels can be introduced to tailor its electronic/optic properties by proper doping.<sup>9,10</sup> Similar to the III-N compounds (such as GaN and AlN), Si<sub>3</sub>N<sub>4</sub> could be an excellent host material in terms of mechanical strength, thermal/chemical stability, and high dopant concentration, thus proving promising for microelectronic/optic devices that can operate at high temperatures and radiation environments. The synthesis of one-dimensional nanostructured Si<sub>3</sub>N<sub>4</sub> has been the subject of several previous studies. Si<sub>3</sub>N<sub>4</sub> nanowires have been synthesized by either confined reaction us-

ing carbon nanotubes as templates<sup>11</sup> or reacting Si and/or SiO<sub>2</sub> with N<sub>2</sub> by heat treatment or combustion with or without catalysts.<sup>12–15</sup> Zhang *et al.*<sup>16</sup> demonstrated that Si<sub>3</sub>N<sub>4</sub> nanowires possess much higher bending strength than the bulk materials. Chen and coworkers synthesized well-aligned silicon nitride nanocones on Si-substrates by plasma-assisted hot-filament CVD.<sup>17</sup> Most recently, Yin *et al.*<sup>18</sup> synthesized silicon nitride nanobelts (rectangular cross-section) via a vapor–solid thermal reaction between ammonia and silicon monoxide.

In this paper, we report the synthesis of Si<sub>3</sub>N<sub>4</sub> nanobelts by catalyst-assisted pyrolysis of a polymeric precursor. Both  $\alpha$ - and  $\beta$ -Si<sub>3</sub>N<sub>4</sub> nanobelts were grown during the confined crystallization of amorphous silicon carbonitride (SiCN), which was obtained by thermal decomposition of a polysilazane precursor. The nanobelts obtained are about 50–100 nm in thickness, 400–1000 nm in width, and several tens of micrometers to several millimeters in length. A growth mechanism based on solid–liquid–gas–solid (SLGS) reaction is proposed. The formation of nanobelts instead of nanowires in this study is attributed to the anisotropy growth of Si<sub>3</sub>N<sub>4</sub> nuclei at an earlier stage. A similar process has been used to synthesize SiC nanorods.<sup>19</sup>

## II. Experimental Procedure

In this study, a commercially available polyureasilazane (Ceraset™, Kion Corporation, Huntingdon Valley, PA) was used as a starting precursor. The as-received Ceraset, which is liquid at room temperature, was first solidified by heat treatment at 260°C for 0.5 h in N<sub>2</sub>.<sup>20</sup> The obtained solid was then crushed into fine powders by high-energy ball milling for 24 h. 3 wt % of FeCl<sub>2</sub> powders (Beijing Bei Hua Fine Chemicals Company Ltd., Beijing, China) was added as catalyst during ball milling. The powder mixture was then placed in a high-purity alumina crucible and pyrolyzed in a conventional furnace with a graphite resistance under flowing ultra-high purity nitrogen of 0.1 MPa. The powder mixture was heated to 1450°C at 10°C/min and held there for 2 h followed by furnace cool. The experiments were also performed on the samples without FeCl<sub>2</sub> additives for comparison.

The morphology, structure, and composition of the pyrolysis products were characterized using field emission scanning electron microscopy (SEM, JSM-6301, JEOL, Tokyo, Japan), X-ray diffraction (XRD, Automated D/Max-RB, Rigaku, Tokyo, Japan) with CuK $\alpha$  radiation ( $\lambda = 1.54178 \text{ \AA}$ ), and high-resolution transmission electron microscope (HRTEM, JEML-2010F, JEOL, Tokyo, Japan) equipped with energy-dispersive spectrum (EDS).

## III. Results and Discussion

The morphology of the Si<sub>3</sub>N<sub>4</sub> nanobelts obtained was first examined using SEM. Figure 1(a) shows a representative SEM

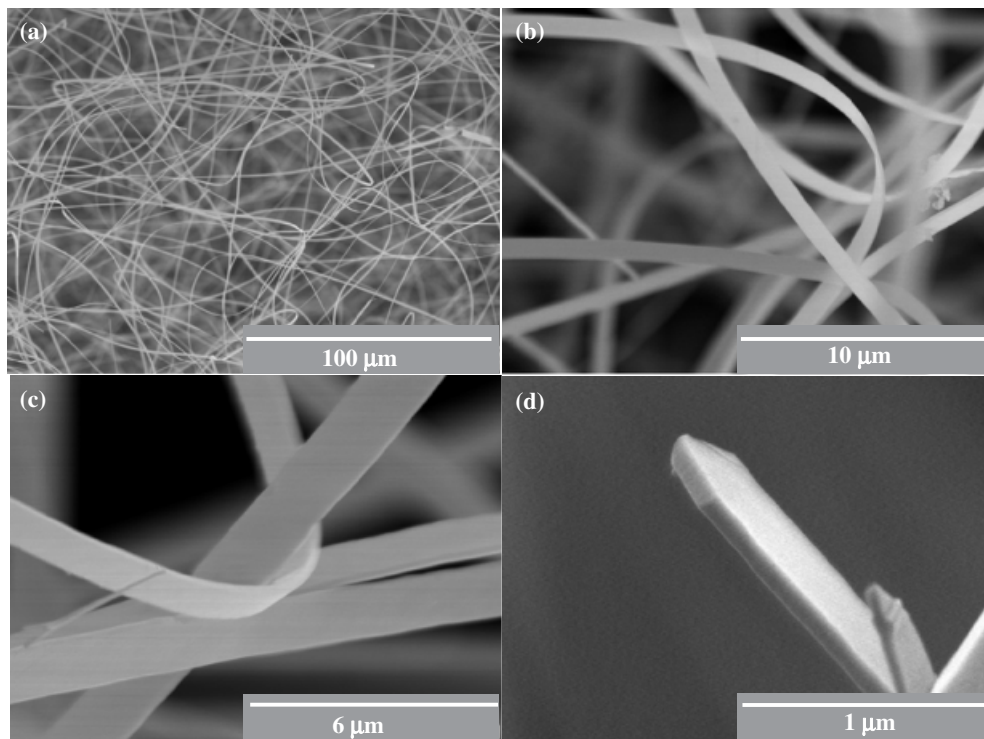
L. C. Klein—contributing editor.

Manuscript No. 10922. Received March 17, 2004; approved July 9, 2004.

Work supported by the National Natural Science Foundation of China (Grant No. 50372031) and “Hundred Person” program of Chinese Academy of Science.

\*Member, American Ceramic Society.

†Address to whom correspondence should be addressed. e-mail: lan@mail.ucf.edu



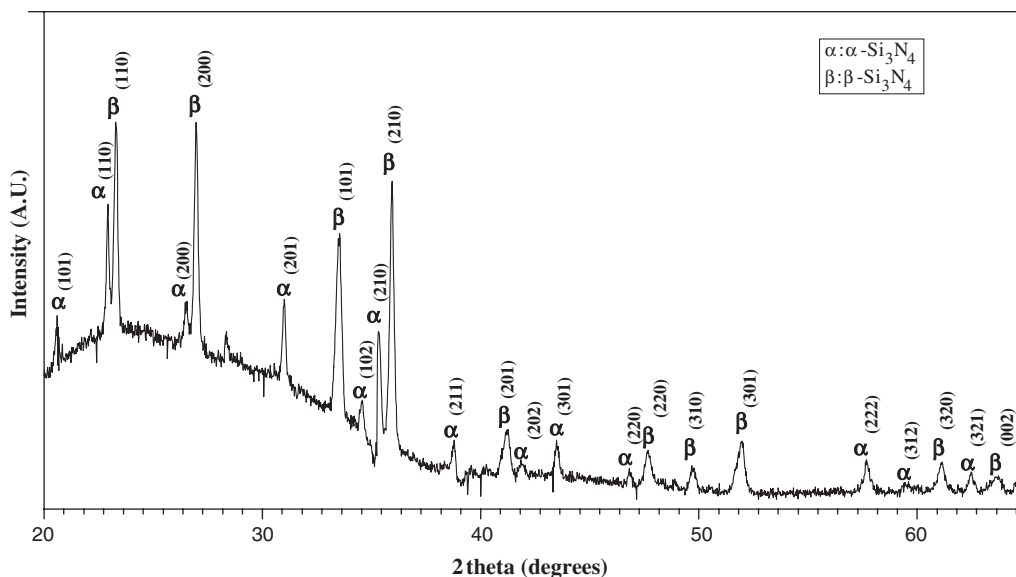
**Fig. 1.** Scanning electron micrographs of  $\text{Si}_3\text{N}_4$  nanobelts: (a) the morphology of the pyrolyzed product under low magnification; (b) and (c) show rectangular cross section of the nanobelts with clean surfaces; (d) shows (i) there are no liquid droplets on the tips of the belts and (ii) the tips take on a triangular shape.

image of the pyrolyzed products, showing that relatively high-density nanobelts have grown homogeneously on the top of the powder matrix. Closer examinations under high magnification (Figs. 1(b) and (c)) reveal that the cross-sections of the  $\text{Si}_3\text{N}_4$  nanostructures are rectangular, 50–100 nm in thickness and 400–1000 nm in width. The lengths of the belts range from a few 100  $\mu\text{m}$  up to several millimeters. Within each individual belt, the thickness and width are uniform along its entire length. The SEM observation also reveals that the surfaces of the belts are smooth and clear without any particles. Most of the nanobelts are highly curved, suggesting they are flexible. Figure 1(d) shows typical image of the tips of the belts. It can be seen from the image that (i) liquid droplets, which are associated with

vapor–liquid–solid (VLS) growth process,<sup>21</sup> are not found at the tips; and (ii) the tips take on a triangular shape, suggesting a significant growth along the width direction at the earlier stage.

The XRD pattern (Fig. 2) of the synthesized nanobelts suggests that pyrolyzed products contain both  $\alpha$ - and  $\beta$ - $\text{Si}_3\text{N}_4$  phases. The broad hump at lower angle regions suggests that the unconverted powders remain amorphous.

Further characterizations of the morphology and crystalline structure of the synthesized nanobelts were carried out by using TEM and HRTEM. Figure 3(a) shows a typical TEM image of both straight and curved portions of  $\text{Si}_3\text{N}_4$  nanobelts. The nanobelts are very thin and highly transparent to electrons; the copper grid can even be seen through the belts. The ripple-like



**Fig. 2.** X-ray diffraction pattern of as-pyrolyzed products suggests the coexistence of  $\alpha$ - and  $\beta$ - $\text{Si}_3\text{N}_4$ .

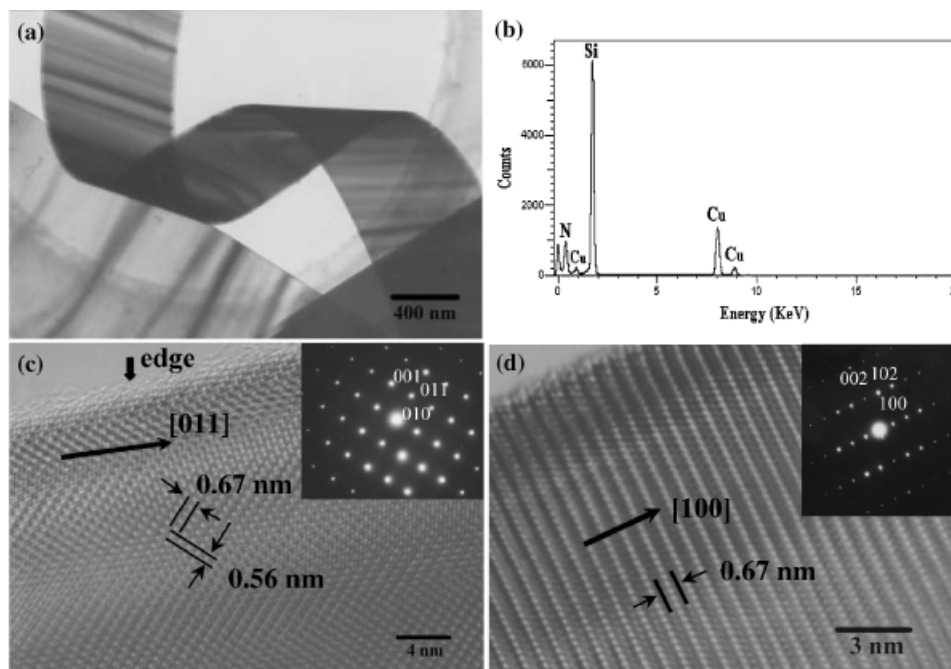


**Fig. 3.** (a) A typical transmission electron microscope image shows both straight and curved parts of the nanobelts; (b) the energy-dispersive spectrum revealed that the belts consist of Si and N elements only; (c) and (d) are high-resolution transmission electron microscope images and corresponding selected area electron diffraction patterns of how the  $\alpha$ - $\text{Si}_3\text{N}_4$  nanobelts grew along [011] and [100] directions, respectively.

contrast is due to the strain resulting from the bending. Note that the density of ripple-like contrast is much higher in the curved portion than in the straight portion. The EDS spectrum in Fig. 3(b) indicates that the nanobelt consists of Si and N elements only (the Cu comes from the copper grid). Figures 3(c) and (d) show typical HRTEM images of the  $\alpha$ - $\text{Si}_3\text{N}_4$  nanobelts with different growth directions. While the XRD pattern suggests their existence,  $\beta$ - $\text{Si}_3\text{N}_4$  nanobelts were not found under HRTEM. The HRTEM images reveal that the nanobelts possess a perfect crystal structure with few defects such as dislocations and stacking faults. The insets show corresponding selected area electron diffraction (SAED) patterns that are identical over the entire belts, indicating that the belts are single crystal. The lattice fringe spacing of 0.56 and 0.67 nm in Fig. 3(c) agrees well with (001) and (010) planes of bulk  $\alpha$ - $\text{Si}_3\text{N}_4$ , where  $a = 0.77541$  nm and  $c = 0.56217$  nm (JCPDS Card No. 41-0360); the lattice fringes of Fig. 3(d) are separated by 0.67 nm, which are the (100) planes of  $\alpha$ - $\text{Si}_3\text{N}_4$ . The lattice fringes and the inserted SAED patterns suggest that the  $\alpha$ - $\text{Si}_3\text{N}_4$  nanobelts grew along both [011] (Fig. 3(c)) and [100] (Fig. 3(d)) directions. The examinations of more than ten belts revealed that [011] and [100] are only growth directions for  $\alpha$ - $\text{Si}_3\text{N}_4$  nanobelts.

No nanobelts were formed in the samples without  $\text{FeCl}_2$  additives, suggesting the catalytic growth of the  $\text{Si}_3\text{N}_4$  nanobelts in this study.

Previous study<sup>20</sup> on the pyrolysis of pure Ceraset without the catalyst revealed that the polysilazane was converted to an amorphous alloy with an apparent composition of  $\text{SiC}_{0.99}\text{N}_{0.84}$  at  $\sim 1000^\circ\text{C}$  under 0.1 MPa  $\text{N}_2$ ; this amorphous phase is retained up to  $\sim 1450^\circ\text{C}$  where it crystallized to  $\text{Si}_3\text{N}_4$  and free carbon. The  $\text{Si}_3\text{N}_4$  and free carbon then reacted with each other to form SiC and  $\text{N}_2$  gas at  $\sim 1500^\circ\text{C}$ . The study clearly suggested that a VLS mechanism,<sup>21</sup> which required Si-containing vapor phase, was not valid in the current study because of the absence of Si-containing vapor phase during the heat-treatment process. Considering these circumstances, we suggest a growth mechanism based on a unique SLGS process for the  $\text{Si}_3\text{N}_4$  nanobelts. At the beginning of the process, the amorphous SiCN reacted with Fe to form a liquid Si-Fe-C alloy at a temperature higher than the eutectic temperature of Si-Fe-C ternary system, and meanwhile released  $\text{N}_2$  gas. Further reaction of the SiCN and

the liquid alloy formed a liquid phase supersaturated with Si and C. This supersaturated liquid phase then reacted with  $\text{N}_2$  gas (at least part of  $\text{N}_2$  was provided by the protection gas) on the liquid/gas interface to precipitate the  $\text{Si}_3\text{N}_4$  nanobelts. The precipitation phase is silicon nitride rather than silicon or silicon carbide because under the pyrolysis conditions, namely  $1450^\circ\text{C}$  and 0.1 MPa  $\text{N}_2$ , the silicon nitride is the most stable phase.<sup>22</sup>

The mechanism that governed the formation of belt-like morphology in the current study is rather difficult to understand; particularly it has been reported<sup>14</sup> that  $\text{Si}_3\text{N}_4$  nanowires with a cross-section close to circle were formed under similar growth conditions at  $1200^\circ\text{C}$ . The only difference between the current research and Kim *et al.*<sup>14</sup> is the heat-treatment temperatures:  $1450^\circ$  and  $1200^\circ\text{C}$ , respectively. The observation of triangle-shaped tips (Fig. 1(d)) suggested a strongly anisotropic growth at an earlier stage. Thereby, we propose the following growth process to account for the formation of nanobelts instead of nanowires: at the beginning of precipitation,  $\text{N}_2$  gas reacts with Si within the supersaturated liquid to form  $\text{Si}_3\text{N}_4$  nuclei; the further growth of the nuclei occurs along the axial direction and width direction simultaneously to form triangle morphology (the growth along width direction only, instead of both width and thickness directions, is due to the anisotropy nature of  $\text{Si}_3\text{N}_4$  crystal structure); the growth along the width direction stops after it reaches a certain value limited by the confining effect of the liquid phase droplets, and further growth only occurs along the axial direction to form nanobelts. A detailed study on the effect of crystalline orientation on anisotropy growth is underway. Accordingly, it is believed that the formation of nanowires instead of nanobelts in Kim *et al.*<sup>14</sup> is because the liquid phase droplets formed at lower temperatures are small and limit the anisotropy growth along the width direction. The temperature dependence of the size of the liquid droplets can be understood by the fact that at higher temperature, more silicon (carbon) can be dissolved in equilibrium liquid phase. The above analysis suggests that we should obtain nanowires at lower temperatures using the same processing procedure.<sup>23</sup>

#### IV. Summary

In summary, ultra-long single-crystalline  $\text{Si}_3\text{N}_4$  nanobelts have been synthesized via catalyst-assisted pyrolysis of a polymer

precursor at 1450°C in 0.1 MPa N<sub>2</sub>. The as-prepared nanobelts are single crystals with a uniform thickness and width, and contain no detectable defects such as dislocations or stacking faults. The thickness and width of Si<sub>3</sub>N<sub>4</sub> nanobelts range from 50 to 100 nm and 400–1000 nm, respectively, and the length is up to several millimeters. The growth directions of  $\alpha$ -Si<sub>3</sub>N<sub>4</sub> nanobelts can be either [011] or [100]. The growth mechanism is a SLGS reaction/crystallization. The formation of nanobelts instead of nanowires in this study is due to the anisotropy growth of Si<sub>3</sub>N<sub>4</sub> nuclei at an earlier stage.

## References

- <sup>1</sup>J. Hu, T. W. Odom, and C. M. Lieber, "Chemistry and Physics in One Dimension: Synthesis and Properties of Nanowires and Nanotubes," *Acc. Chem. Res.*, **32**, 435–45 (1999).
- <sup>2</sup>Y. Xia, P. Yang, Y. Sun, Y. Wu, B. Mayers, B. Gates, Y. Yin, F. Kim, and H. Yan, "One-Dimensional Nanostructures: Synthesis, Characterization, and Applications," *Adv. Mater.*, **15**, 353–89 (2003).
- <sup>3</sup>L. An, W. Xu, S. Rajagopalan, C. Wang, H. Wang, Y. Fan, L. Zhang, D. Jiang, J. Kapat, L. Chow, B. Guo, J. Liang, and R. Vaidyanathan, "Carbon Nanotube Reinforced Polymer-Derived Ceramic Composites," *Adv. Mater.*, **16** [22], 2036–40 (2004).
- <sup>4</sup>M. Kazes, D. Y. Lewis, Y. Ebenstein, T. Mokari, and U. Banin, "Lasing from Semiconductor Quantum Rods in a Cylindrical Microcavity," *Adv. Mater.*, **14**, 317–21 (2002).
- <sup>5</sup>X. Duan, Y. Huang, R. Agarwal, and C. M. Lieber, "Single-Nanowire Electrically Driven Lasers," *Nature*, **421**, 241–5 (2003).
- <sup>6</sup>M. Scheffler, P. Greil, A. Berger, E. Pippel, and J. Woltersdorf, "Nickel-Catalyzed *in situ* Formation of Carbon Nanotubes and Turbostratic Carbon in Polymer-Derived Ceramics," *Mater. Chem. Phys.*, **84**, 131–9 (2004).
- <sup>7</sup>G. Ziegler, J. Heinrich, and C. Wötting, "Relationships Between Processing, Microstructure and Properties of Dense and Reaction-Bonded Silicon-Nitride," *J. Mater. Sci.*, **22**, 3041–86 (1987).
- <sup>8</sup>R. K. Govila, "Strength Characterization of Yttria-Doped Sintered Silicon-Nitride," *J. Mater. Sci.*, **20**, 4345–53 (1985).
- <sup>9</sup>F. Munakata, K. Matsuo, K. Furuya, Y. J. Akimune, and I. Ishikawa, "Optical Properties of beta-Si<sub>3</sub>N<sub>4</sub> Single Crystals Grown from a Si Melt in N<sub>2</sub>," *Appl. Phys. Lett.*, **74**, 3498–500 (1999).
- <sup>10</sup>A. R. Zanatta and L. A. O. Nunes, "Green Photoluminescence from Er-Containing Amorphous SiN Thin Films," *Appl. Phys. Lett.*, **72**, 3127–9 (1998).
- <sup>11</sup>W. Han, S. Fan, Q. Li, B. Qu, and D. Yu, "Synthesis of Silicon Nitride Nanorods Using Carbon Nanotube as a Template," *Appl. Phys. Lett.*, **71**, 2271–3 (1997).
- <sup>12</sup>X. Wu, W. Song, B. Zhao, W. Huang, M. Pu, Y. Sun, and J. Du, "Synthesis of Coaxial Nanowires of Silicon Nitride Sheathed with Silicon and Silicon Oxide," *Solid State Commun.*, **115**, 683–6 (2000).
- <sup>13</sup>Y. Zhang, N. Wang, R. He, J. Liu, X. Zhang, and J. Zhu, "A Simple Method to Synthesize Si<sub>3</sub>N<sub>4</sub> and SiO<sub>2</sub> Nanowires from Si or Si/SiO<sub>2</sub> Mixture," *J. Cryst. Growth*, **233**, 803–8 (2001).
- <sup>14</sup>H. Kim, J. Park, and H. Yang, "Synthesis of Silicon Nitride Nanowires Directly from the Silicon Substrates," *Chem. Phys. Lett.*, **372**, 269–74 (2003).
- <sup>15</sup>H. Chen, Y. Cao, X. Xiang, J. Li, and C. Ge, "Fabrication of  $\beta$ -Si<sub>3</sub>N<sub>4</sub> Nanofibers," *J. Cryst. Growth*, **325**, L1–3 (2001).
- <sup>16</sup>Y. Zhang, N. Wang, R. He, Q. Zhang, J. Zhu, and Y. Yan, "Reversible Bending of Si<sub>3</sub>N<sub>4</sub> Nanowire," *J. Mater. Res.*, **15**, 1048–51 (2000).
- <sup>17</sup>Y. Chen, L. Guo, and D. T. Shaw, "High-Density Silicon and Silicon Nitride Cones," *J. Cryst. Growth*, **210**, 527–31 (2000).
- <sup>18</sup>L. Yin, Y. Bando, Y. Zhu, and Y. Li, "Synthesis, Structure, and Photoluminescence of Very Thin and Wide Alpha Silicon Nitride ( $\alpha$ -Si<sub>3</sub>N<sub>4</sub>) Single-Crystal-line Nanobelts," *Appl. Phys. Lett.*, **83**, 3584–6 (2003).
- <sup>19</sup>W. Yang, H. Miao, Z. Xie, L. Zhang, and L. An, "Synthesis of Silicon Carbide Nanorods by Catalyst-Assisted Pyrolysis of Polymeric Precursor," *Chem. Phys. Lett.*, **383** [1–2] 441–4 (2004).
- <sup>20</sup>Y. Li, E. Kroke, R. Riedel, C. Fasel, C. Gervais, and F. Babonneau, "Thermal Cross-linking and Pyrolytic Conversion of Poly(ureamethylvinyl)silazanes to Silicon-based Ceramics," *Appl. Organometal. Chem.*, **15**, 820–32 (2000).
- <sup>21</sup>R. S. Wagner and W. C. Ellis, "Vapor-Liquid-Solid Mechanism of Single Crystal Growth," *Appl. Phys. Lett.*, **4**, 89–90 (1964).
- <sup>22</sup>H. J. Seifert, J. Peng, H. L. Lucas, and F. Aldinger, "Phase Equilibria and Thermal Analysis of Si-C-N Ceramics," *J. Alloys Comp.*, **320** [2] 251–61 (2001).
- <sup>23</sup>W. Yang, H. Miao, Z. Xie, L. Zhang, and L. An, "Synthesis of Silicon Nitride Nanowires by Catalyst-Assisted Pyrolysis of Polymeric Precursor," *J. Am. Ceram. Soc.* (in press).

□